Carbohydrate Polymers 111 (2014) 744–752

Contents lists available at ScienceDirect

Carbohydrate Polymers

journal homepage: www.elsevier.com/locate/carbpol

Preparation and immunomodulating activities of a library of low-molecular-weight α-glucans

Rui Zhu [1], Xian Zhang [1], Wei Liu, Yan Zhou, Ran Ding, Wenbing Yao *, Xiangdong Gao *

State Key Laboratory of Natural Medicines, School of Life Science and Technology, China Pharmaceutical University, Nanjing, Jiangsu, PR China

ARTICLE INFO

Article history:
Received 26 January 2014
Received in revised form 10 April 2014
Accepted 30 April 2014
Available online 21 May 2014

Keywords:
Low-molecular-weight glucan
Immunomodulation
Functional unit
Acid degradation
Toll-like receptor

ABSTRACT

YCP, an α-D-glucan with molecular weight of 2.4×10^3 kDa, was isolated from the mycelium of marine fungus *Phoma herbarum* YS4108. It interacted with TLR2 and TLR4 to induce B cells proliferation and activation. Here, a series of homogenous LMWYCPs (namely LMWYCP-1 to LMWYCP-6) were obtained by acid degradation. LMWYCP-3 and LMWYCP-4 were capable of inducing the proliferation of B cells dramatically. Further research involved TLR defunctionalization and competitive binding assay demonstrated that the immunomodulating activities of LMWYCP-4 was TLR4-dependent but TLR2-independent, while that mediated by LMWYCP-3 was neither TLR2- nor TLR4-dependent. Together with the structural information that LMWYCPs shared the similar structure features with YCP, we deduced that LMWYCP-4 may be the functional unit of YCP responsible for YCP/TLR4 interaction. This is the first time that the probable functional unit of glucan with the structure of α-D-(1–4)-linked residues in main chain and α-D-(1–6)-linked residues in branches is reported.

1. Introduction

In current decades, much attention has been attracted to polysaccharides in the field of biochemistry and pharmacology because of their multiple bioactivities and pharmacological actions, such as immunological, anti-tumor, anti-virus and anti-oxidation activities (Yang & Zhang, 2009). As one kind of biomacromolecules, the bioactivities of polysaccharides are tightly dependent on their structures including monosaccharide composition and sequence, glucosidic bonds, configuration and chain conformations (Chi, Chen, Wang, Xiong, & Li, 2008; Rudd et al., 2010; Yang & Zhang, 2009). Hence, the investigation of the structure–activity relationship (SAR) of polysaccharides has always been the focus of glycobiology researchers. Back in the 1990s, the SAR of β-(1–3)-glucans had been investigated in detail (Bohn & BeMiller, 1995). Until recently, related research still garnered a lot of attention (Zhang, Li, Wang, Zhang, & Cheung, 2011; Zhang, Li, Xu, & Zeng, 2005). Furthermore, served as the basic polymer, β-(1–3)-glucans were chemically modified with sulfate donor to examine the correlation of anticoagulant activities and the degree of sulfation as well as the molecular weight (Franz & Alban, 1995). However, specialized studies involved the SAR of α-glucans were seldom introduced. This situation indeed has been an obstacle for the further development of this kind of polysaccharides.

YCP, an α-glucan isolated from the mycelium of *Phoma herbarum* YS4108, was composed of α-D-(1–4)-linked glucose residues, with branches at C-6 consisting of non-reducing terminal approximately every seventeen residues (Yang et al., 2005). This polysaccharide has great potential in inhibiting the growth of tumors (Heps, S180 and Lewis) without bringing any abnormal behavior of the experiment mice (Chen, Guo, Gao, & Qian, 2005). Further researches demonstrated that the anti-tumor activity of YCP was greatly attributed to its modulation of the host innate and adaptive immune responses such as enhancement of the phagocytic activity of macrophages, promotion of the proliferation of lymphocytes as well as induction of cytokine secretion. Further studies on the immunomodulating mechanism of YCP revealed that some members of Toll-like receptor (TLR) family, including TLR2 and TLR4, were responsible for YCP functions on B cells (Chen et al., 2009; Yang et al., 2005; Zhang et al., 2013). Despite all these advances, it remained unclear about the SAR of YCP, particularly in terms of the unit of YCP required for its immunomodulating activities (so-called functional unit). Thus, related studies could not only enhance the understanding of YCP as an efficacious biological response modifier in oncologic immunotherapy, but provide us the information which may be of particular value in understanding the relationship of structure and activity of α-glucans.

* Corresponding authors. Tel.: +86 25 83271543; fax: +86 25 83271543.
E-mail addresses: wbyao@cpu.edu.cn (W. Yao), xdgao@cpu.edu.cn (X. Gao).
[1] Both authors contributed equally to this paper.

http://dx.doi.org/10.1016/j.carbpol.2014.04.106
0144-8617/

Acidic or enzymatic-catalyzed hydrolysis has always been employed to depolymerize macromolecular polysaccharides to provide a library of oligosaccharides or low-molecular-weight saccharide analogs for screening the functional units of original polysaccharide ligands (Hu, Liu, Wang, & Ding, 2009; Ikeda et al., 2011; Jin et al., 2011; Wang et al., 2012). In the present study, in order to further understand the molecular mechanism underlying the immunomodulating activity of YCP and expand our knowledge in the SAR of α-glucans, we utilized trifluoroacetic acid (TFA) to hydrolyze YCP to prepare a series of low-molecular-weight fragments. Since our previous study has demonstrated the requirement of TLR2 and TLR4 for YCP-mediated B cell activation, we then evaluated the immunomodulating properties of each low-molecular-weight YCP (LMWYCP) on B cells and investigated whether they were functionally related to TLR2 and TLR4 signaling. On this basis, we nicely correlated the activities of LMWYCPs with the molecular size and discussed the probable functional unit of YCP for its immunomodulating activity.

2. Materials and methods

2.1. Materials and animals

The polysaccharide YCP was purified from the mycelium of marine filamentous fungus *P. herbarum* YS4108 following the protocols described previously (Yang et al., 2005). Bio Gel P-10 gel, medium (Bio-Rad, America) were purchased from HanBang Biotech Co., Ltd., Nanjing, China. T-series dextran standards were purchased from Pharmacia Co. Ltd., (Uppsala, Sweden). RPMI-1640 medium and FCS were obtained from Gibco (Grand Island, NY, USA). 3-(4,5-dimethylthiazol-2-yl)-2,5-diphenyl-tetrazolium bromide (MTT), lipopolysaccharide (LPS), fluoresceinamine (FLA) and 1-cyano-4-dimethylaminopyridine tetrafluoroborate (CDAP) were from Sigma–Aldrich (St. Louis, MO, USA). The column of Shodex SUGAR KS-805 (8.0 mm × 300 mm) was from YMC. Co., Ltd. (Kyoto, Japan). TFA and all of other chemicals and reagents were analytical grade.

BALB/c mice between 6 and 8 weeks old were provided by the Experimental Animal Center of Yangzhou University (Yangzhou, Jiangsu, China). B6.129-Tlr2$^{tm1Kir/J}$ (TLR2-KO) and C57BL/10ScNJ (TLR4-KO) mice between 6 and 8 weeks old were provided by the Model Animal Research Center of Nanjing University (Nanjing, Jiangsu, China). All mice were housed in a specific pathogen-free (SPF) facility under normal laboratory conditions, i.e., room temperature (22 ± 2 °C), 45–55% relative humidity, and 12/12 h light–dark cycle with free access to standard rodent chow and water.

2.2. Preparation of LMWYCPs

2.2.1. Partial hydrolysis, isolation and purification of LMWYCPs

The LMWYCPs were obtained by acid degradation. In detail, YCP (60 mg) was dissolved and partially hydrolyzed in TFA solution at a concentration of 10 mg per milliliter in an ampoule. Reaction was terminated by removing the tube from the water bath and the acid remaining in products was removed by repeated evaporations with methanol. After dissolved in distilled water, the hydrolysate was fractioned on a Bio Gel P-10 column (1.6 cm × 100 cm) and eluted with deionized water at a flow rate of 0.125 ml/min. Fractions (1.5 ml each tube) were gathered, and sugar content was monitored by the phenol–sulfuric acid method at 490 nm. After collecting the specific part of the eluent, six crude LMWYCPs with higher content were obtained, which were further purified by another Bio-Gel P-10 column with the same parameters stated above after accumulation respectively. Then the collected fractions were concentrated and lyophilized to give six white LMWYCPs.

The main affecting factors of acid hydrolysis of YCP were the concentration of TFA, reaction time and temperature. In order to optimize the hydrolysis conditions, single-factor test was designed and developed with the ratio of the target area (area between 10.0 min and 11.5 min in HPLC spectrum of hydrolysate which corresponded to the molecular weight from pan- to kilo-Da) as a reference. The details of the reaction conditions were given in Section 3.1.

2.2.2. Measurement of molecular weight and distribution

The molecular weights of LMWYCPs were determined by high-performance gel permeation chromatography (HPGPC) equipped with a pump (LC-20AT, SHIMADZU), a column (Shodex SUGAR KS-805) and a refractive index detector (RID-10A, SHIMADZU). The column temperature was kept at 30 °C while detector was 35 °C. All samples were dissolved in distilled water and passed through a 0.22 μm Millipore filter. Then 20 μl solutions were loaded on the column and eluted with deionized water with flow rate of 0.8 ml/min. *T*-series dextrans were used as standards to calibrate the column.

2.3. Immunomodulating activity of LMWYCPs

2.3.1. Isolation of murine B cells

Murine spleens were gently homogenized in RPMI-1640 medium. Erythrocytes were lysed by NH_4Cl hypotonic buffer (Tris 2.6 g/l, NH_4Cl 7.47 g/l, pH 7.2), and adherent cells were removed by adherence selection overnight in complete medium (RPMI-1640 supplemented with 10% FCS, 60 mg/l penicillin and 100 mg/l streptomycin). The non-adherent cells were enriched, and B cell fraction was isolated from them using a nylon fiber column (Wako, Osaka, Japan) following the manufacturer's instructions. Cells that were $CD19^+$ were identified as B cells through fluorescence-activated cell sorting (FACS).

2.3.2. B-cell proliferation assay

Splenic B cells were isolated from BALB/c, B6.129-Tlr2$^{tm1Kir/J}$ and C57BL/10ScNJ mice as described above. B cells were seeded into 96-well plates at a density of 4×10^6 cells/ml in complete RPMI-1640 medium (100 μl). YCP and LMWYCPs at final concentration of 200 μg/ml, unless otherwise stated, were added to wells (100 μl) and incubated for 48 h at 37 °C. B-cell proliferative response was detected by incubation of cells with MTT (5 mg/ml) for 4 h, followed by addition of DMSO for 10 min. Absorbance was measured at 570 nm in a multiskan spectrum (Thermo Fisher Scientific, Vantaa, Finland), and induction of cell proliferation was expressed as the proliferation index, calculated by dividing A_{570} of stimulated cells with A_{570} of control cells.

2.3.3. Competitive binding assay

Fluoresceinamine-labeled YCP (fl-YCP) was prepared using the CDAP-activation method as previously described (Zhang et al., 2013). Unlabeled YCP-degraded derivatives at concentration of 4000 μg/ml were mixed with 250 μg/ml of fl-YCP, respectively, and incubated with 1×10^5 B cells in 200 μl PBS containing 1% BSA for 1 h on ice. Free fl-YCP and YCP-degraded derivatives in the supernatants were removed by two washes, and cells were collected for FACSCalibur analysis. Data was acquired from a minimum of 1×10^5 cells using the CellQuest Pro program (BD Bioscience) and analyzed by the FlowJo program (FreeStar, Ashland, OR, USA).

2.4. Structure identification of LMWYCPs

2.4.1. FT-IR analysis

The infrared spectrums (IR) of YCP and LMWYCPs were recorded by a Nicolet-170X spectrophotometer in the range of 4000–400 cm^{-1} using the KBr-disk method.

2.4.2. NMR analysis

^{1}H NMR and ^{13}C NMR spectrums were recorded by Brucker AVIII-500 NMR Spectrometer at 30 °C. D_2O was used as the solvent.

2.4.3. Methylation and GC–MS analysis

The methylation analysis was performed according to the method of Needs and Selvendran (1993). Complete methylation was confirmed by the disappearance of the O—H absorption band (3100–3700 cm^{-1}) in FT-IR spectrum. The permethylated products were hydrolyzed subsequently by HCOOH (88%) for 6 h at 100 °C and then TFA (2 M) for 8 h at 100 °C. The partially methylated sugars in the hydrolysate were reduced by $NaBH_4$ and acetylated (Sweet, Shapiro, & Albersheim, 1975). The resulting alditol acetates were analyzed by GC–MS (model: 6890N-5975B, Agilent, USA) with an HP-5MS quartz capillary column (30 m × 0.25 mm × 0.25 μm). Temperature program was set rising from 160 °C up to 180 °C at 1 °C/min then up to 220 °C (standing for 10 min) at 3 °C/min. Range of mass charge ratio (m/z) was 25–500.

The degrees of branching (DB) of LMWYCP-3, LMWYCP-4 and YCP were calculated based on the following formula:

$$CB = \frac{N_T + N_B}{N_T + N_B + N_L}$$

in which N_T, N_B, and N_L were the mol% of terminal residues, branched residues, and linear residues, respectively (Bae et al., 2013; Hawker, Lee, & Frechet, 1991).

2.5. Statistical analysis

The Prism 5.0 program (GraphPad Software, La Jolla, CA, USA) was used for statistical analysis. Student's t-test or ANOVA were performed to determine significant differences where appropriate.

3. Results

3.1. Effects of TFA concentration, reaction time and temperature on YCP hydrolysis

Concentration of TFA, reaction time and temperature are three key parameters that may influence the process of YCP hydrolysis and the resultant production of LMWYCPs. Here, concentration of TFA was set at 15.6, 31.3, 62.5, 125, 250, 500 and 1000 mM to investigate its effect on the hydrolysis of YCP while other reaction conditions were as follows: reaction time 1 h and temperature 100 °C. As shown in Fig. 1A, there was an increasing trend in the proportion of target LMWYCPs from 15.6 to 62.5 mM where the proportion achieved a maximum percentage of 46%. After this point, the proportion decreased obviously. Therefore, 62.5 mM was selected as the optimal concentration of TFA in the following experiments. Reaction time was set at 15, 30, 45, 60, 90, 120 and 150 min when other hydrolysis conditions were similar to those described above. From Fig. 1B, we found that the proportion of target LMWYCP increased from 33% to 45% as the reaction time increased from 15 to 45 min. When the hydrolysis duration was longer than 45 min, the proportion dropped slightly. Thus, 45 min is most favorable reaction time for production of target LMWYCPs. As to reaction temperature, it was set at 50, 60, 70, 80, 90, 100 and 110 °C with the other two conditions determined above. As shown in Fig. 1C, YCP was rarely hydrolyzed by TFA when the temperature below 70 °C. The proportion of target LMWYCPs increased with keeping increasing of temperature, and reached the highest at 100 °C. We thereby chose 100 °C as the optimal reaction temperature.

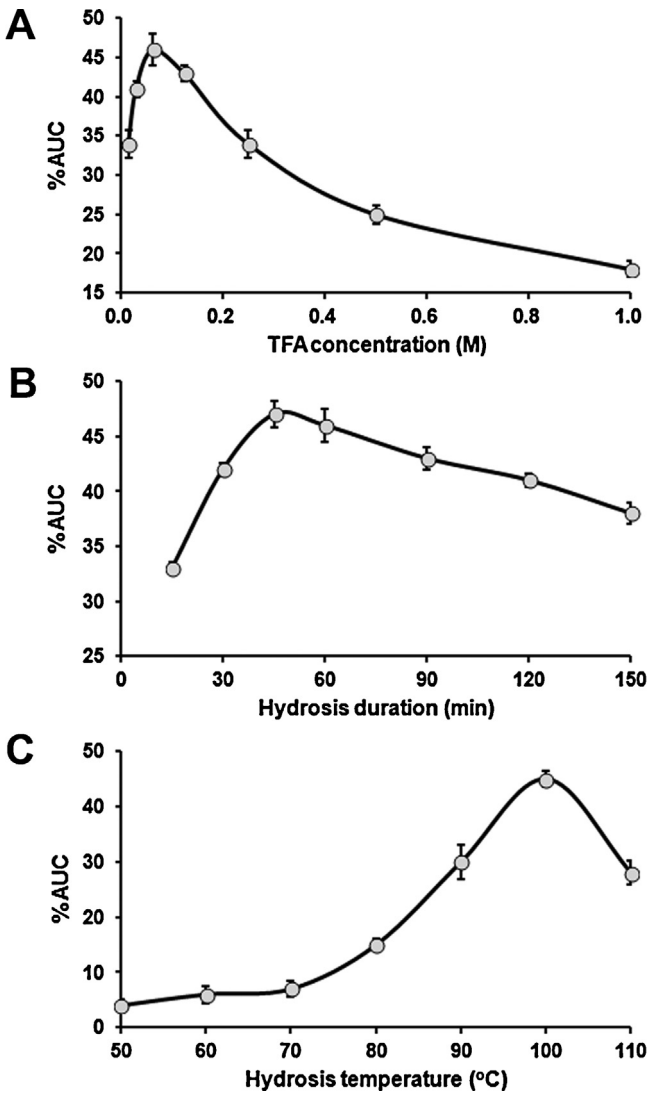

Fig. 1. Effects of TFA concentration, reaction time and temperature on YCP hydrolysis. The hydrolysis products of YCP obtained with different reaction conditions were analyzed on a Shimadzu HPLC system equipped with a Shodex SUGAR KS-805 column and a refractive index detector. The ratio of areas under the curve (AUC) of the goal products with the corresponding TFA concentration, reaction time and temperature are shown in A, B and C respectively.

3.2. Purification of LMWYCPs

The acid hydrolysis products of YCP were separated by size-exclusion chromatography on a Bio Gel P-10 column. Each fraction of the crude LMWYCP, in the same conditions, was sequentially carried to the second purification in accordance with the average molecular weight from largest to smallest after the first purification. Fig. 2A showed six eluting peaks arranged from left to right. In every separation profile, a single eluting peak with small prominence behind can be observed. After collecting the top of each eluting peaks followed by concentration and lyophilization, six LMWYCPs, respectively named LMWYCP-1, LMWYCP-2, LMWYCP-3, LMWYCP-4, LMWYCP-5 and LMWYCP-6 were obtained.

3.3. Determination of molecular weight and purity

HPGPC is the most popular method for determining the molecular weight of polymers (Gómez-Ordóñez, Jiménez-Escrig,

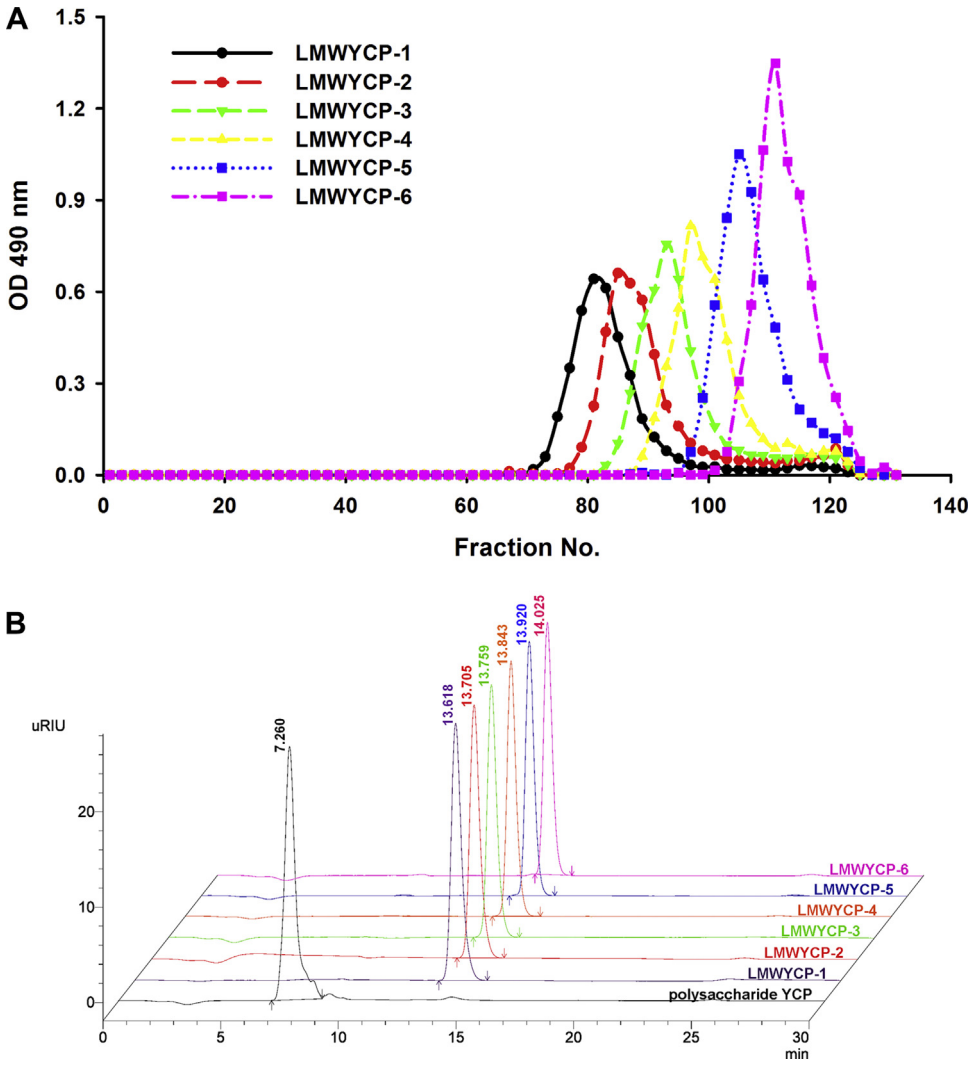

Fig. 2. (A) Bio-Gel P-10 eluting curves of LMWYCPs. The hydrolysis product of YCP obtained under the optimum conditions was fractionated on a Bio-Gel P-10 column. Each fraction with a volume of 7.5 ml was collected, concentrated, and further purified by another Bio-Gel P-10 column with distilled H_2O as the eluent. The eluting curves of different fractions on the second Bio-Gel P-10 column are shown. (B) HPGPC analysis of YCP and LMWYCPs. YCP and LMWYCPs were analyzed on a Shimadzu HPLC system equipped with a Shodex SUGAR KS-805 column and a refractive index detector. The HPLC spectra of YCP and each LMWYCP with the corresponding retention time (T_R) are shown.

& Rupérez, 2012; Nguyen, Winnik, & Buschmann, 2011). Analogous analysis of α-glucans with the similar structure features of YCP were successfully carried out in recent years (Shi et al., 2012; Yan et al., 2013). Using a series of standard dextrans (molecular weight: 1000 Da, 2500 Da, 4600 Da, 7100 Da, and 10,000 Da) as references, the relative molecular weights of LMWYCP-1, LMWYCP-2, LMWYCP-3, LMWYCP-4, LMWYCP-5 and LMWYCP-6 were estimated to be 4664 Da, 3834 Da, 3409 Da, 2819 Da, 2339 Da and 1841 Da, respectively. All the six LMWYCPs showed a single and symmetrically sharp peak on HPLC (Fig. 2B), and their polydispersity indexes, the indicator of polymer homogeneity, were approximately 1 (Table 1). These observations indicated that the six LMWYCPs possessed a high purity and good homogeneity, and each of them could be used for subsequent functional testing.

Table 1
Average molecular weight and distribution of LMWYCPs from HPGPC.

LMWYCP	Retention time (min)	M_w (Da)	M_n (Da)	M_w/M_n [a]	DP[b]
LMWYCP-1	13.618	4664	3484	1.33	28.7
LMWYCP-2	13.705	3834	2934	1.30	23.6
LMWYCP-3	13.759	3409	2704	1.26	20.9
LMWYCP-4	13.843	2819	2281	1.23	17.3
LMWYCP-5	13.920	2339	1947	1.20	14.3
LMWYCP-6	14.025	1841	1541	1.19	11.3

Calibration curve: $y = -1.016x + 17.512$, $r = 0.993$. x = retention time (min), $y = \log M_w$, r = correlation coefficient.
[a] Polydispersity index.
[b] Degree of polymerization.

3.4. Immunomodulating activity of LMWYCPs

The effects of six LMWYCPs on B cell proliferation were shown in Fig. 3A. Among these LMWYCPs, LMWYCP-3 and LMWYCP-4, albeit less potent than YCP, were capable of inducing the proliferation of B cells dramatically, whereas the other four did not show any detectable proliferative effect at all the doses tested. Moreover, LMWYCP-4 seemed to be more effective than LMWYCP-3 since it can dose-dependently stimulate B cells to proliferative while this manner did not appear in LMWYCP-3-treated cells.

In our previous study, TLR2 and TLR4 signaling have been identified to be responsible for the immunomoduating activity of YCP in B cells (Zhang et al., 2013). Given that both LMWYCP-3 and LMWYCP-4 were structurally analog to YCP, it is highly possible

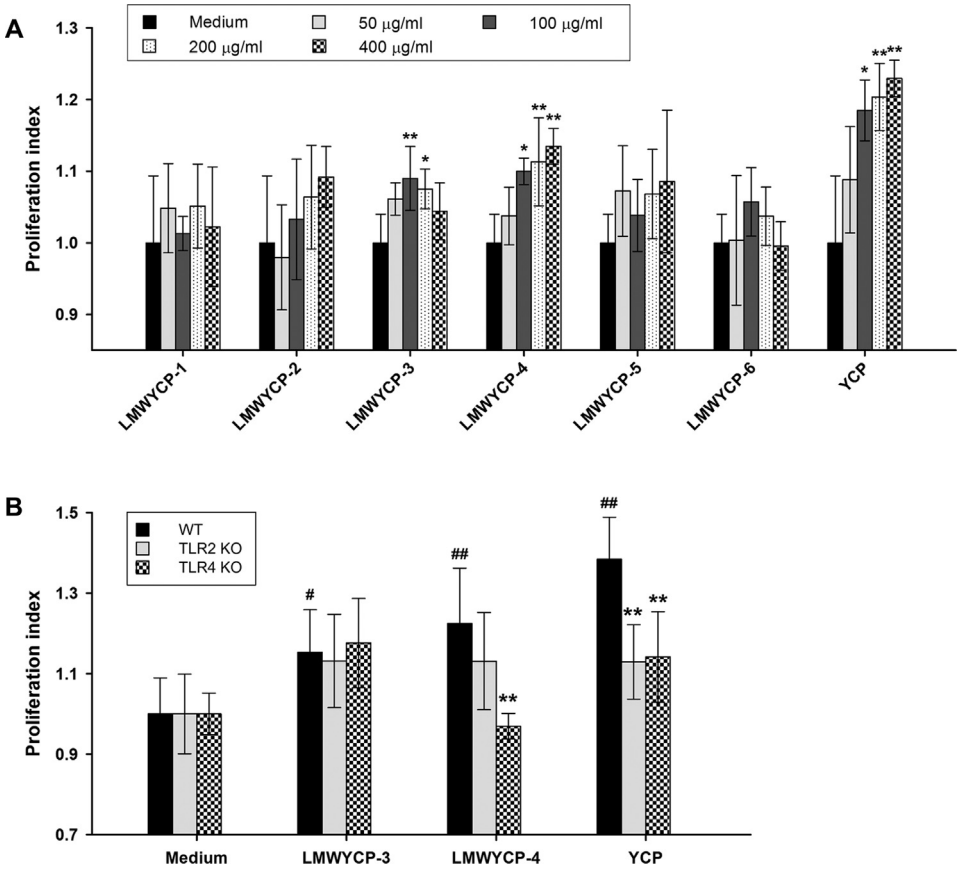

Fig. 3. Effects of LMWYCPs on B cell proliferation. (A) Proliferative responses of WT B cells to LMWYCPs. Splenic B cells were treated with different LMWYCPs or YCP at the indicated concentrations for 48 h, and then subjected to proliferation test by MTT assay ($n = 6$, $^{*}p \leq 0.05$, $^{**}p \leq 0.01$ vs. medium by Kruskal–Wallis test followed by Dunn's post hoc test). (B) Effect of TLR2 and TLR4 defunctionalization on the proliferative effects of LMWYCP-3 and LMWYCP-4. B cells from WT, TLR2 and TLR4 KO mice were stimulated with 200 μg/ml of LMWYCP-3 and LMWYCP-4 and YCP, respectively, for 48 h, and then assayed for cell proliferation ($n = 6$, $^{**}p \leq 0.01$ vs. WT, $^{\#}p \leq 0.05$, $^{\#\#}p \leq 0.01$ vs. Medium by Mann–Whitney *U* test).

that the two LMWYCPs also mediated the immunostimulation of B cells through a TLR2- and/or TLR4-dependent mechanism. To confirm this hypothesis, the impact that loss of TLR2 and TLR4 has upon LMWYCP-3 and LMWYCP-4 activities was investigated in B cells from either B6.129-Tlr2$^{tm1Kir/J}$ (TLR2-KO) or C57BL/10ScNJ (TLR4-KO) mice. As indicated in Fig. 3B, knocking-out of TLR4 allele significantly reduced the proliferative effects of LMWYCP-4 and YCP on B cells when compared with the wide-type controls. However, such reduction was not found in the TLR4-deficient B cells treated with LMWYCP-3. In the analogous proliferation test using TLR2-KO B cell compartment, it was found that TLR2 deficiency only impaired the B-cell proliferative responses to YCP rather than its degraded derivatives LMWYCP-3 and LMWYCP-4. Taken together, these findings suggested that the induction of proliferation by LMWYCP-4 was TLR4-dependent but TLR2-independent, while that mediated by LMWYCP-3 was neither TLR2- nor TLR4-dependent.

To further confirm the statement obtained in B-cell proliferation assay, competitive binding assay was further performed to examine the direct binding capacity of LMWYCPs to B cells. To begin with, wide-type B cells were incubated with fl-YCP in the presence of excess unlabeled LMWYCPs (16-fold amount of fl-YCP) for 1 h and then subjected to flow cytometric analysis. Among all the six LMWYCPs, only additional LMWYCP-4 decreased the median fluorescent intensity of B cells by 37% when compared with LMWYCP-free control, suggesting LMWYCP-4 may share, at least partly, an overlapping receptor profile with YCP. Since the proliferation assay revealed the functional relevance of TLR4 rather than TLR2 in LMWYCP-4-mediated B cell responses, we next investigated the inhibitory effect of LMWYCP-4 on YCP binding in TLR2- or TLR4-KO B cells. As expected, LMWYCP-4 were still capable of inhibiting the binding of YCP to TLR2-KO B cells as in the case with wide-type cells, but failed to induce a similar effect on TLR4-KO B cell compartment, implying the receptor profile of LMWYCP-4 includes TLR4 but excludes TLR2. By contrast, LMWYCP-3 did not result in any significant inhibition on YCP binding to either TLR2- or TLR4-KO B cells (Fig. 4). This provided the evidence that LMWYCP-4 could specifically bind to TLR4, whereas the binding ability of LMWYCP-3 toTLR2 or TLR4 was absent.

Combining Figs. 3 and 4 together, we proposed that LMWYCP-4 may be the functional unit of YCP responsible for YCP:TLR4 interaction. In addition, LMWYCP-3 probably utilized a TLR2- and TLR4-independent signaling to activate B cells since both its binding and proliferative effect did not require functional TLR2 and TLR4.

3.5. FT-IR analysis and NMR analysis

The FT-IR and NMR analysis were used for the structure characterization of LMWYCP-3 and LMWYCP-4. Fig. 5A showed a strong band near 3400 cm^{-1} assigned to the hydroxyl stretching vibration. The weak band at 2900 cm^{-1} attributed to C—H stretching vibration and the band at 1650 cm^{-1} corresponded to bound water. The bands in the region of 850 and 930 cm^{-1} indicated the α-configuration of the sugar units (Barker, Bourne, Stacey, & Whiffen, 1954). Three peaks at 1150, 1080 and 1025 cm^{-1} also suggested the presence of α-pyranose of the glucose residue and bands at 1025 cm^{-1} and 1080 cm^{-1}, a characteristic of link type, indicated

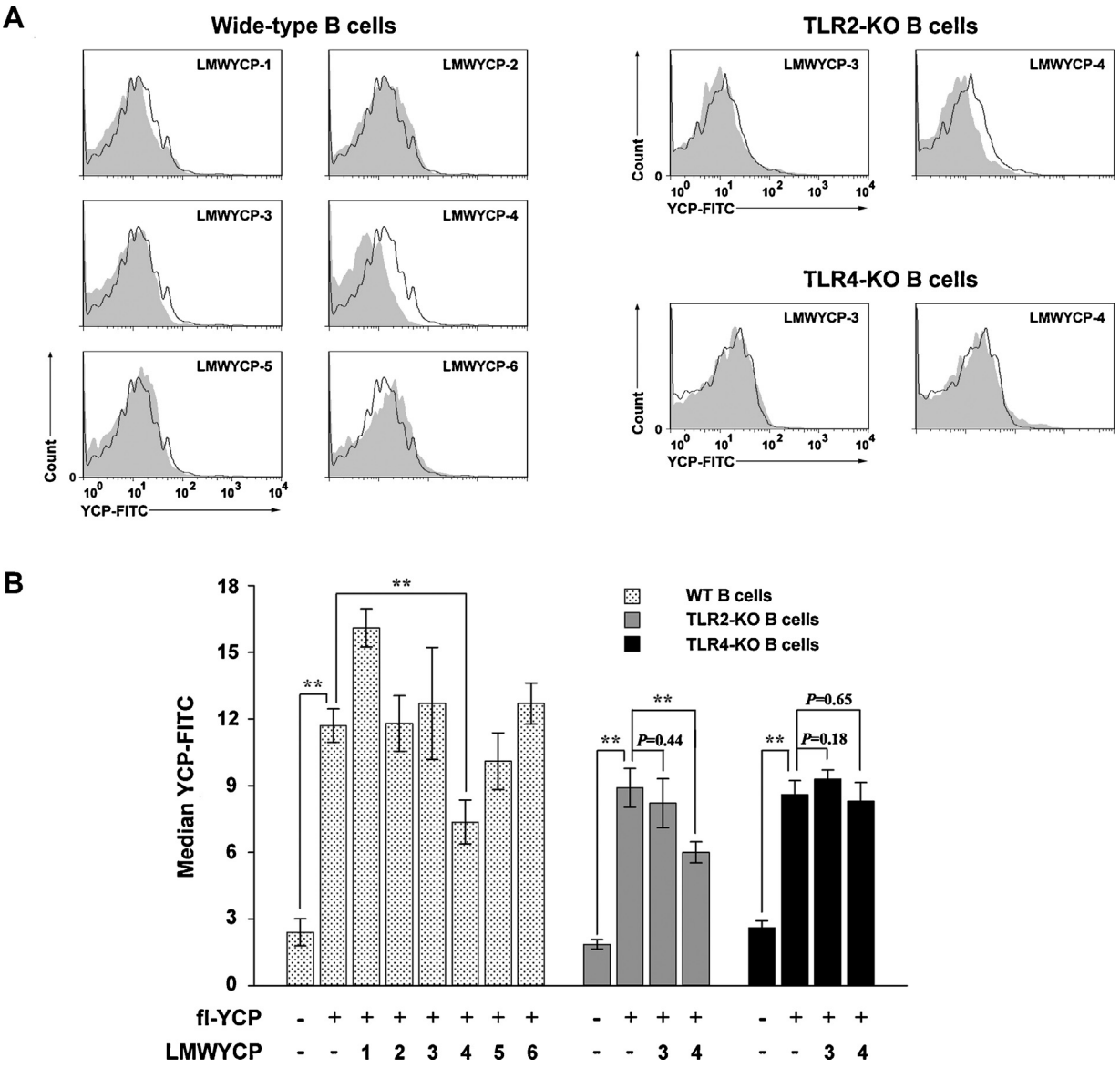

Fig. 4. Competitive inhibition of fl-YCP binding to B cells by LMWYCPs. B cells from wide-type, TLR2- and TLR4-KO mice were incubated with 250 μg/ml of fl-YCP for 1 h in the presence of LMWYCP-1, LMWYCP-2, LMWYCP-3, LMWYCP-4, LMWYCP-5, or LMWYCP-6, respectively, at concentrations of 4000 μg/ml, and then harvested for flow cytometric analysis. The histogram overlays shown in panel A are representative of triplicates, and the quantitative data expressed as median fluorescence intensity are presented in panel B. For each plot in panel A, the open histogram represents staining of cells by fl-YCP in the absence of LMWYCPs (LMWYCP-free), while the filled gray histogram represents fl-YCP binding in the presence of the indicated LMWYCP.

the α-(1→6) and α-(1→4) linkages both existed in the two YCP-degraded derivatives (Shingel, 2002). All the characteristic peaks can be observed in the IR spectrum of YCP. Overall the IR data suggested that the depolymerization of YCP by TFA did not change the basic chemical structure of YCP molecules.

This suggestion was further evidenced by the NMR spectrums of LMWYCP-3, LMWYCP-4 and YCP (Fig. 5B and C). Though it is difficult to clearly assign all the proton signals of samples overlap in the range of 3.5–5.5 ppm in the ^{1}H NMR spectrum (Fig. 5B), three anomeric proton signals at ~5.0, 5.4, 5.3 ppm corresponded to residues A (α-D-Glcp-(1→), B (→4)-α-D-Glc*p*-(1→) and C (→4,6)-α-D-Glc*p*-(1→) were obvious. According to the integration data of the peak areas, three types of residues in LMWYCP-3, LMWYCP-4 and YCP were respectively in the ratio of nearly 1.4:9.2:1, 1.2:6.6:1 and 1.3:16.3:1. In ^{13}C NMR spectrum, the range of the chemical shifts of samples is much wider than that of ^{1}H chemical shift. It is able to provide us more information about the fine chemical structures of saccharides. As shown in Fig. 5C, the signals at ~100 ppm corresponded to the anomeric carbon of Glc residues. The signals at ~76 ppm corresponded to the C-4 carbons of residues B, C and reducing end unit. The signals at ~60 ppm were assigned to the unlinked C-6 carbons of all the residues except the branching point unit. The other signals distributed in the region of 68–75 ppm were attributed respectively to the C-2, C-3, C-5 carbons in all the residues, the C-4 carbons in residues A, the C-6 carbons in residues C and the reducing end unit. Combined with the ^{13}C NMR spectroscopic assignments for α-D-glucans (Chen et al., 2011; Ishurd et al., 2010; Ni et al., 2009; Shi et al., 2012; Yan, Wang, Li, & Wu, 2011), we concluded that both LMWYCP-3 and LMWYCP-4 shared the same primary structure with YCP, i.e., a linear α-(1→4) bonded glucopyranoside main chain lightly substituted with a few α-(1→6)-linked side chain (Yang et al., 2005).

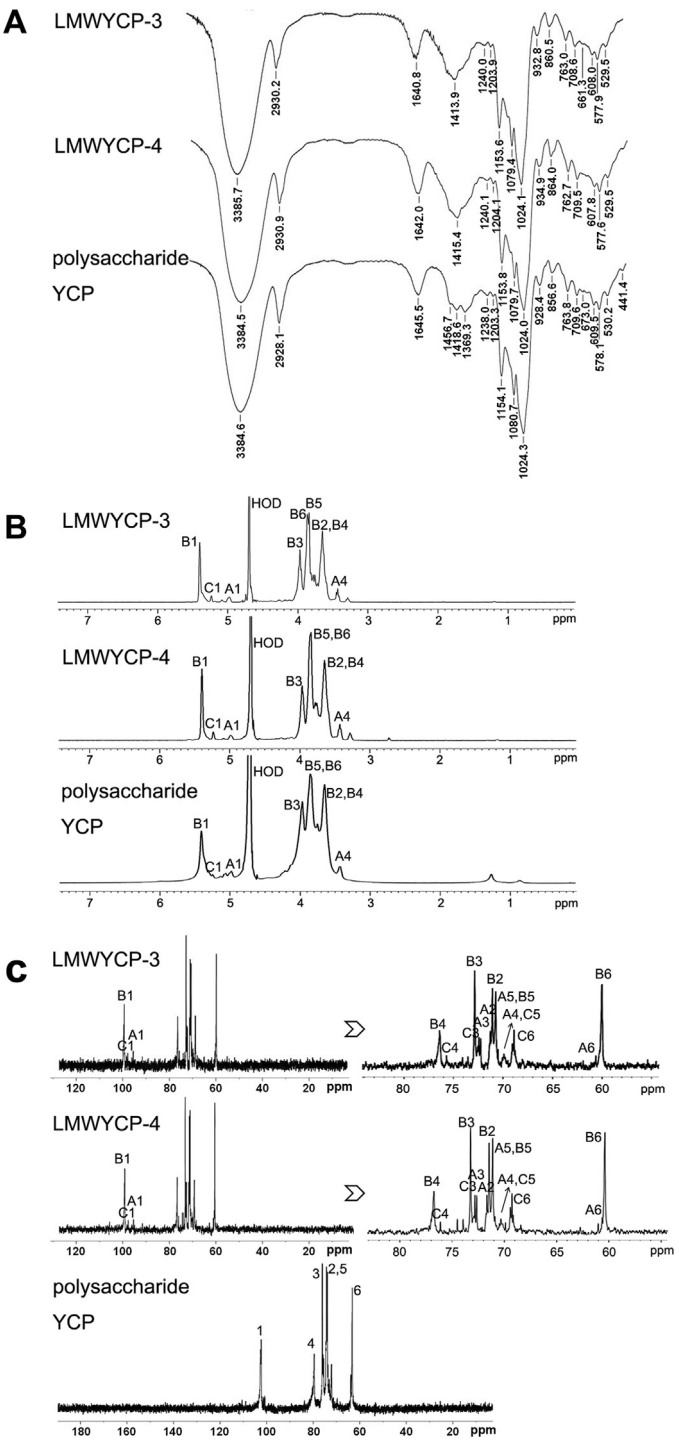

Fig. 5. (A) FT-IR, (B) ^{1}H NMR and (C) ^{13}C NMR spectras of LMWYCP-3, LMWYCP-4 and YCP.

3.6. Methylation and GC–MS analysis

To further characteristic the detailed structure of LMWYCP-3 and LMWYCP-4, methylation and GC-MS assay were performed. The results (Table 2) indicated that the backbone chains of YCP and its' two degradation products were all mainly (1→4)-linked-α-D-glucopyranosyl (Residue-B) and (1→4, 6)-linked-α-D-glucopyranosyl residues (Residue-C). The side chain attached to the O-6 position of Residue-C contained single non-reducing terminal (1→)-α-D-glucopyranosyl (Residue-A) group. According to the integration data of the peak areas, residues of A, B and C in LMWYCP-3, LMWYCP-4 and YCP were respectively in the ratio of 1.2:8.9:1, 1.3:6.3:1 and 1:16.1:1. This was also in accordance with the results of the NMR analysis. Besides, the DB of LMWYCP-3, LMWYCP-4 and YCP calculated based on the results above were 19.8%, 26.7% and 11.0%, respectively.

Table 2
Results of methylation analysis of LMWYCP3, LMWYCP-4 and YCP.

Methylated sugar[a]	Type of linkage	Retention time (min)	Molar ratios[b]
LMWYCP-3			
2,3,4,6-Me$_4$-Glc	α-D-Glcp-(1→	9.78	1.2
2,3,6-Me$_3$-Glc	→4)-α-D-Glc*p*-(1→	13.43	8.9
2,3-Me2-Glc	→4,6)-α-D-Glc*p*-(1→	18.29	1
LMWYCP-4			
2,3,4,6-Me$_4$-Glc	α-D-Glcp-(1→	9.76	1.3
2,3,6-Me$_3$-Glc	→4)-α-D-Glc*p*-(1→	13.51	6.3
2,3-Me2-Glc	→4,6)-α-D-Glc*p*-(1→	18.31	1
YCP			
2,3,4,6-Me$_4$-Glc	α-D-Glcp-(1→	9.83	1
2,3,6-Me$_3$-Glc	→4)-α-D-Glc*p*-(1→	13.55	16.1
2,3-Me2-Glc	→4,6)-α-D-Glc*p*-(1→	18.34	1

[a] 2,3,4,6-Me$_4$-Glc = 1,5-tri-acetyl-2,3,4,6-tri-O-methyl glucitol, etc.
[b] Relative molar ratio, calculated from the ratio of peak areas.

4. Discussion

In this study, acidic hydrolysis was employed to obtain a library of LMWYCPs to investigate the structure–activity relationship of YCP. Compared with the enzyme degradation which incised sugar chain at specific points and brought fragments with approximate molecular weight (Ren, Yan, Yao, Jin, & Gao, 2010), acidic hydrolysis of YCP could produce a series of fragments with different molecular weight by the control of reaction conditions. In addition, in weak acid solution, the hydrolysis of glycosides likely acted as described by Holtan, Zhang, Strand, and Skjåk-Bræk (2006) and by Yan et al. (2009), resulting fragments with the similar primary structure to YCP. This was in accordance with our results from the structure analysis of LMWYCPs.

In our single-factor test for optimizing hydrolysis conditions (Fig. 1), the largest proportion of target LMWYCPs was obtained in the following reaction conditions: TFA concentration 62.5 mM, reaction time 45 min and reaction temperature 100 °C. The results did not mean the lessening of degradation after the optimal point but for the further diminished of products' molecular weights caused by the YCP's deeply degradation, which might bring too much fragments with extreme low molecular weight and reduced the proportion of objective LMWYCPs.

Given that the primary structure of LMWYCPs was similar to YCP (Fig. 5 and Table 2), the difference of DP/molecular size in six LMWYCPs might partly attribute to the disparity in activity. Therefore, the relationship of proliferation index and DP of LMWYCP was analyzed (Fig. 6). It was found that the immunostimulatory activity of LMWYCP increased as the DP value diminished from 29 to 17, and decreased rapidly when DP reduced continually. It could be deduced that the fragment with about 17 residues might comprise a basic functional unit of YCP responsible for the induction of TLR4-dependent B cell activation. Supernumerary glucose unit might shelter the functional region and weaken the bioactivity, while sugar chain shorter than 17 residues might not be enough to maintain the conformation of the functional unit and caused the loss of the activity as well. Actually, similar conclusion about the relation between the DP and biological function of sugar chain could be found in many reports. Bland, Keshavarz, and Bucke (2004) found that the activation on immune cells of araban and cyclodextrin differed with the degree of polymerization. As the DP of the arabino-oligosaccharides increased from 6

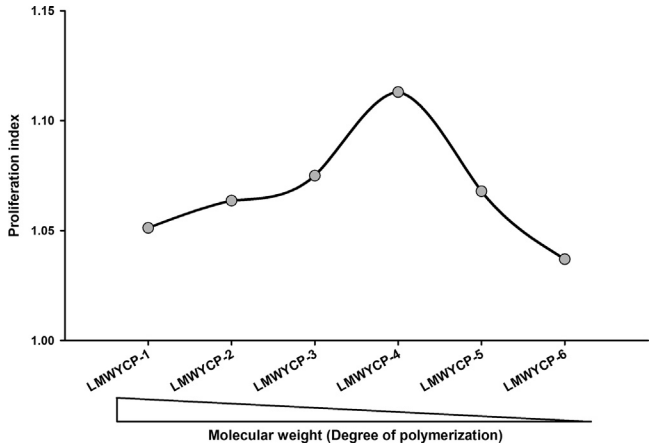

Fig. 6. The relationship between the proliferative effect at 200 μg/ml and molecular size (degree of polymerization) of LMWYCP.

to 8, ROS (reactive oxidizing species) production by immune cells decreased, while β-cyclodextrin with DP of 7 was more inhibitory than α-cyclodextrin (DP 6) and γ-cyclodextrin (DP 8). Laminariheptaose, another important oligosaccharide, had been determined as the smallest functional unit recognized by macrophage glucan receptors (Lowe et al., 2001). Combined this conclusion with the discovery that Laminariheptaose could complete a rotation in the secondary structure (Bland et al., 2004), it was easy to find that the suitable DP/molecular size of sugar chain played an important role in the formation of conformation which was required for the recognition by specific receptors. Actually, with the ChemBio-Draw software, Hu and coworkers (Hu et al., 2009) investigated the difference of conformation of three oligosaccharides with DP of 5, 6 and 11 respectively. Models showed that compared with the conformation (a more flattened pocket structure) of pentasaccharide, one additional galactose unit altered the conformation and caused the loss of the bioactivity, whereas, undecasaccharide composed of the part of five residues and a deeper pocket structure formed by the other six residues exhibited pronounced biological activities. Taken together, the bioactivity of saccharide could be influenced by the DP through the expanding molecular length as well as the higher structure emerged in specific environment. Our study demonstrated LMWYCP-4 with about 17 glucose residues might be the functional unit of YCP responsible for the induction of TLR4-dependent B cell activation, which indicated for the first time the functional unit of glucan with the structure of α-D-(1–4)-linked residues in main chain and α-D-(1–6)-linked residues in branches. Though the impact of DP/molecular size on bioactivity had been studied, the branches' effective still unclear, which should be further researched.

It was noteworthy that LMWYCP-3 and LMWYCP-4 were structurally similar but elicited the B cell responses via different pathway. LMWYCP-4 activated B cells through TLR4 but not TLR2 while LMWYCP-3 exerted its immunostimulating activity through a TLR2 and TLR4-independent mechanism (Figs. 3 and 4). However, as their mother compound, YCP activated immunocytes through TLR2 and TLR4 synthetically (Zhang et al., 2013). Similarly, other studies focusing on the immune receptors of α-glucans also brought us some interesting findings. For instance, ESG, an α-1, 6-branched a-1,4-glucan prepared by enzymatically synthesized, emerged its immunomodulating activity through TLR2 but not TLR4 (Kakutani, Adachi, Takata, Kuriki, & Ohno, 2012), and another α-glucan isolated from *Pseudallescheria boydii* cell wall induced cytokine secretion by innate immunocytes through a TLR2-involved mechanism as well (Bittencourt et al., 2006). However, α-glucan derived from *M. tuberculosis* activated immunocytes through DC-SIGN which belonged to C-type lectin receptors (Geurtsen et al., 2009). On this basis, we proposed that polysaccharides even though sharing the similar primary structure might utilize different receptors to activate immunocytes. This diversity of receptor profiles in the face of similar backbones may be attributed to the difference in the fine structure among these polysaccharides, such as molecular size/DP, degree of branching and branching length. In addition, the three-dimensional conformation of polysaccharides might also account for the diversity in their respective receptor profile.

5. Conclusions

In this report, six homogeneous LMWYCPs named LMWYCP-1 to LMWYCP-6 with average molecular weights of 4664 Da, 3834 Da, 3409 Da, 2819 Da, 2339 Da and 1841 Da, respectively, were obtained by the acidic degradation of YCP. Proliferative effects of LMWYCPs on B cells were investigated and two derivates, LMWYCP-3 and LMWYCP-4, exhibited significant bioactivities. Further research involved TLR defunctionalization and competition assay indicated that the induction of proliferation by LMWYCP-4 was TLR4-dependent but TLR2-independent, while that mediated by LMWYCP-3 was neither TLR2- nor TLR4-dependent. Further structure characterization demonstrated that the structural features of LMWYCP-4 were very similar to YCP. Taken together, our findings has for the first time suggested that LMWYCP-4 with a DP value of about 17 may be the functional unit of YCP responsible for its interaction with TLR4 and subsequent TLR4-dependent B cell activation.

Acknowledgements

This study was mainly supported by the National Natural Science Foundation of China (81072570, 31301473), the National Scientific and Technological Major Project for Significant New Drugs Creation (No. 2012ZX09502001-004), the Innovative Scientific Research Team Fund of Jiangsu Province, the Specialized Research Fund for the Doctoral Program of Higher Education (20100096110004), the Ph.D. Programs Foundation of Ministry of Education of China (CXZZ11_0820), and the Fundamental Research Funds for the Central Universities (JKPZ2013014).

References

Bae, I. Y., Kim, H. W., Yoo, H. J., Kim, E. S., Lee, S., Park, D. Y., et al. (2013). Correlation of branching structure of mushroom β-glucan with its physiological activities. *Food Research International*, *51*, 195–200.

Barker, S. A., Bourne, E. J., Stacey, M., & Whiffen, D. H. (1954). Infrared spectra of carbohydrates. Part I. Some derivatives of D-glucopyranose. *Journal of the Chemical Society*, *1*, 171–176.

Bittencourt, V. C. B., igueiredo, R. T., Silva, R. B., Mourao-Sá, D. S., Fernandez, P. L., Sassaki, G. L., et al. (2006). An α-glucan of *Pseudallescheria boydii* is involved in fungal phagocytosis and Toll-like receptor activation. *Journal of Biological Chemistry*, *281*, 22614–22623.

Bland, E. J., Keshavarz, T., & Bucke, C. (2004). The influence of small oligosaccharides on the immune system. *Carbohydrate Research*, *339*, 1673–1678.

Bohn, J. A., & BeMiller, J. N. (1995). (1→3)-β-D-Glucans as biological response modifiers: A review of structure-functional activity relationships. *Carbohydrate Polymers*, *28*, 3–14.

Chen, S., Yin, D. K., Yao, W. B., Wang, Y. D., Zhang, Y. R., & Gao, X. D. (2009). Macrophage receptors of polysaccharide isolated from a marine filamentous fungus *Phoma herbarum* YS4108. *Acta Pharmacologica Sinica*, *30*(7), 1008–1014.

Chen, X., Cao, D., Zhou, L., Jin, H., Dong, Q., Yao, J., et al. (2011). Structure of a polysaccharide from *Gastrodia elata* Bl., and oligosaccharides prepared thereof with anti-pancreatic cancer cell growth activities. *Carbohydrate Polymers*, *86*, 1300–1305.

Chen, Z., Guo, Q., Gao, X., & Qian, Z. (2005). Tumor inhibitory effect of YCP (a marine fugal polysaccharide) (I). *Chinese Journal of Natural Medicines*, *13*, 396–400.

Chi, A. P., Chen, J. P., Wang, Z. Z., Xiong, Z. Y., & Li, Q. X. (2008). Morphological and structural characterization of a polysaccharide from *Gynostemma Pentaphyllum* Makino and its anti-exercise fatigue activity. *Carbohydrate Polymers*, *74*, 868–874.

Franz, G., & Alban, S. (1995). Structure–activity relationship of antithrombotic polysaccharide derivatives. *International Journal of Biological Macromolecules*, *17*, 311–314.

Geurtsen, J., Chedammi, S., Mesters, J., Cot, M., Driessen, N. N., Sambou, T., et al. (2009). Identification of mycobacterial α-glucan as a novel ligand for DC-SIGN: Involvement of mycobacterial capsular polysaccharides in host immune modulation. *Journal of Immunology*, *183*, 5221–5231.

Gómez-Ordóñez, E., Jiménez-Escrig, A., & Rupérez, P. (2012). Molecular weight distribution of polysaccharides from edible seaweeds by high-performance size-exclusion chromatography (HPSEC). *Talanta*, *93*, 153–159.

Hawker, C., Lee, R., & Frechet, J. (1991). One-step synthesis of hyperbranched dendritic polyesters. *Journal of the American Chemical Society*, *113*, 4583–4588.

Holtan, S., Zhang, Q., Strand, W. I., & Skjåk-Bræk, G. (2006). Characterization of the hydrolysis mechanism of polyalternating alginate in weak acid and assignment of the resulting MG-oligosaccharides by NMR spectroscopy and ESI-mass spectrometry. *Biomacromolecules*, *7*, 2108–2121.

Hu, K., Liu, Q., Wang, S., & Ding, K. (2009). New oligosaccharides prepared by acid hydrolysis of the polysaccharides from *Nerium indicum* Mill and their anti-angiogenesis activities. *Carbohydrate Research*, *344*, 198–203.

Ikeda, Y., Charef, S., Ouidja, M. O., Barbier-Chassefière, V., Sineriz, F., Duchesnay, A., et al. (2011). Synthesis and biological activities of a library of glycosaminoglycans mimetic oligosaccharides. *Biomaterials*, *32*, 769–776.

Ishurd, O., Zgheel, F., Elghazoun, M., Elmabruk, M., Kermagi, A., Kennedy, J. F., et al. (2010). A novel (1→4)-α-D-glucan isolated from the fruits of *Opuntia ficus indica* (L.) Miller. *Carbohydrate Polymers*, *82*, 848–853.

Jin, M., Iwamoto, T., Yamada, K., Satsu, H., Totsuka, M., & Shimizu, M. (2011). Effects of chondroitin sulfate and its oligosaccharides on Toll-like receptor-mediated IL-6 secretion by macrophage-like J774.1 cells. *Bioscience Biotechnology and Biochemistry*, *7*, 1283–1289.

Kakutani, R., Adachi, Y., Takata, H., Kuriki, T., & Ohno, N. (2012). Essential role of Toll-like receptor 2 in macrophage activation by glycogen. *Glycobiology*, *22*, 146–159.

Lowe, E., Rice, P., Ha, T., Li, C., Kelley, J., Ensley, H., et al. (2001). A (1→3)-β-D-linked heptasaccharide is the unit ligand for glucan pattern recognition receptors on human monocytes. *Microbes and Infection*, *3*, 789–797.

Needs, P. W., & Selvendran, R. R. (1993). Avoiding oxidative degradation during sodium hydroxide/methyl iodide-mediated carbohydrate methylation in dimethyl sulfoxide. *Carbohydrate Research*, *245*, 1–10.

Nguyen, S., Winnik, F. M., & Buschmann, M. D. (2011). Improved reproducibility in the determination of the molecular weight of chitosan by analytical size exclusion chromatography. *Carbohydrate Polymers*, *83*, 1997–2004.

Ni, W., Zhang, X., Bi, H., Iteku, J., Ji, L., Sun, C., et al. (2009). Preparation of a glucan from the roots of *Rubus crataegifolius* Bge. and its immunological activity. *Carbohydrate Research*, *344*, 2512–2518.

Ren, M., Yan, W., Yao, W., Jin, L., & Gao, X. (2010). Enzymatic degradation products from a marine polysaccharide YCP with different immunological activity and binding affinity to macrophages, hydrolyzed by α-amylases from different origins. *Biochimie*, *92*, 411–417.

Rudd, T. R., Skidmore, M. A., Guerrini, M., Hricovini, M., Powell, A. K., Siligardi, G., et al. (2010). The conformation and structure of GAGs: Recent progress and perspective. *Current Opinion in Structural Biology*, *20*, 567–574.

Shi, Y., Zhao, L., Liu, X., Hu, F., Cui, F., Bi, Y., et al. (2012). Structural characterization of a sulfated glucan isolated from the aqueous extract of *Hedysarum polybotrys* Hand.-Mazz. *Carbohydrate Polymers*, *87*, 160–169.

Shingel, K. I. (2002). Determination of structural peculiarities of dextran, pullulan and γ-irradiated pullulan by Fourier-transform IR spectroscopy. *Carbohydrate Research*, *337*, 1445–1451.

Sweet, D. P., Shapiro, R. H., & Albersheim, P. (1975). Quantitative analysis by various g.l.c. Response-factor theories for partially methylated and partially ethylated alditol acetates. *Carbohydrate Research*, *40*, 217–225.

Wang, W., Zhang, P., Yu, G. L., Li, C. X., Hao, C., Qi, X., et al. (2012). Preparation and anti-influenza A virus activity of κ-carrageenan oligosaccharide and its sulphated derivatives. *Food Chemistry*, *133*, 880–888.

Yan, J. K., Li, L., Wang, Z. M., Leung, P. H., Wang, W. Q., & Wu, J. Y. (2009). Acidic degradation and enhanced antioxidant activities of exopolysaccharides from *Cordyceps sinensis* mycelial culture. *Food Chemistry*, *117*, 641–646.

Yan, J. K., Wang, W. Q., Li, L., & Wu, J. Y. (2011). Physiochemical properties and antitumor activities of two α-glucans isolated from hot water and alkaline extracts of Cordyceps (Cs-HK1) fungal mycelia. *Carbohydrate Polymers*, *85*, 753–758.

Yan, W., Niu, Y., Lv, L., Xie, Z., Jin, L., Yao, W., et al. (2013). Characterization of a heteropolysaccharide isolated from diploid *Gynostemma pentaphyllum* Makino. *Carbohydrate Polymers*, *92*, 2111–2117.

Yang, L., & Zhang, L. M. (2009). Chemical structural and chain conformational characterization of some bioactive polysaccharides isolated from natural sources. *Carbohydrate Polymers*, *76*, 349–361.

Yang, X. B., Gao, X. D., Han, F., Xu, B. S., Song, Y. C., & Tan, R. X. (2005). Purification, characterization and enzymatic degradation of YCP, a polysaccharide from marine filamentous fungus *Phoma herbarum* YS4108. *Biochimie*, *87*, 747–754.

Zhang, L., Li, X., Xu, X., & Zeng, F. (2005). Correlation between antitumor activity, molecular weight, and conformation of lentinan. *Carbohydrate Research*, *340*, 1515–1521.

Zhang, X., Ding, R., Zhou, Y., Zhu, R., Liu, W., Jin, L., et al. (2013). Toll-like receptor 2 and Toll-like receptor 4-dependent activation of B cells by a polysaccharide from marine fungus *Phoma herbarum* YS4108. *PLoS ONE*, *8*, 1–11.

Zhang, Y., Li, S., Wang, X., Zhang, L., & Cheung, P. C. (2011). Advances in lentinan: Isolation, structure, chain conformation and bioactivities. *Food Hydrocolloids*, *25*, 196–206.